Title

EFFECTS OF SURFACE DISORDER, VARIOUS SURFACE STRUCTURES OF CHEMISORBED GASES AND CARBON ON HELIUM ATOMIC BEAM SCATTERING FROM THE (100) SURFACE OF PLATINUM

Authors

West, L.A.
Somorjai, G.A.

Publication Date

1970-10-01

Submitted to Journal of
Chemical Physics

UCRL-20357
Preprint

c. 2

EFFECTS OF SURFACE DISORDER, VARIOUS SURFACE STRUCTURES OF CHEMISORBED GASES AND CARBON ON HELIUM ATOMIC BEAM SCATTERING FROM THE (100) SURFACE OF PLATINUM

L. A. West and G. A. Somorjai

October 1970

AEC Contract No. W-7405-eng-48

LAWRENCE RADIATION LABORATORY
UNIVERSITY of CALIFORNIA BERKELEY

UCRL-20357

c. 2

DISCLAIMER

EFFECTS OF SURFACE DISORDER, VARIOUS SURFACE STRUCTURES OF CHEMISORBED GASES AND CARBON ON HELIUM ATOMIC BEAM SCATTERING FROM THE (100) SURFACE OF PLATINUM

L. A. West[†] and G. A. Somorjai

Inorganic Materials Research Division, Lawrence Radiation Laboratory
Department of Chemistry, University of California
Berkeley, California 94720

ABSTRACT

Low energy electron diffraction and helium atomic beam scattering have been combined to investigate on the (100) face of a platinum single crystal the effects of changing surface structure on the gas-solid interaction. The angular distribution of a helium beam scattered from the ordered and disordered crystal face has been monitored. The intensity of the specularly scattered beam increases by nearly an order of magnitude upon atomic ordering of the metal surface. Ordered domains of graphitic carbon also yielded high specular intensities. The magnitude of the intensity maxima for helium beams scattered from ordered surface structures of various chemisorbed gases (CO, C_2H_2) was sensitive to surface order but insensitive to the type of surface structure formed. For all the surface structures studied the scattered helium beam distribution was directed with the intensity maximum at the specular angle. The surface temperature dependence of the scattered specular intensity was monitored in the temperature range 450°K to 1300°K. Anomalous changes in the beam intensity could be associated with the adsorption of carbon monoxide on the crystal face.

I. INTRODUCTION

Of the different gases used in gas-solid scattering experiments, helium atomic beams appear to undergo the weakest interaction with the surface. The fraction of the incident beam scattered specularly (i.e. the incident and scattering angles are equal) has been reported to be as large as 25% in some instances.[1] This is at least an order of magnitude greater than the specular fraction observed with other atomic beams. Such a weak interaction is not at all surprising in view of the small size, large ionization energy, and small polarizability of the helium atom. If one defines a "reduced" energy for the gas-solid interaction as $\epsilon = \Delta H_{ads}/RT_g$ where ΔH_{ads} is the heat of adsorption of the gas on a given surface, R is the universal gas constant, and T_g is the gas "temperature"*, ϵ is approximately unity for helium at 300°K on most solid surfaces because of its small heat of adsorption ($\leq$ 2 kcal/mole for many solids). For other rare gases the reduced interaction energies are much larger due to their larger heats of adsorption. Despite its weak interaction with the surface however, the helium beam was found to be very sensitive to surface contamination. Whether ordered or disordered, adsorbed impurities present to the incoming helium atoms a scattering surface having physical characteristics (i.e. atomic weight, dimensions and force constants) quite different from those of the clean surface. Specular intensities were found to be markedly reduced by the presence of adsorbed gas atoms on the surface.

---

*The "temperature" of a molecular beam is only a meaningful quantity if the velocity distribution of the beam is represented by some well defined function of the source temperature. For low pressure effusion from a Knudsen cell, $T_g = T_{source}$. However, for high pressure flow from a Knudsen cell, multichannel array, or nozzle source, the beam's velocity distribution is no longer of the simple Maxwell-Boltzman type and one must either define a beam temperature through a functional relationship with a measured beam velocity or use the true beam energy in place of RT_g in the expression for ϵ.

In this paper we report on combined helium atomic beam scattering and low energy electron diffraction (LEED) studies of the (100) face of a platinum single crystal. The characteristics of the scattered beams were monitored as a function of the surface temperature and of the atomic order of the surface. LEED patterns were correlated with the observed angular distributions for helium beam scattering from a variety of ordered surface structures of different chemisorbed species.

Helium beam scattering was found to be very sensitive to atomic disorder on the surface and only slightly sensitive to the nature of the different ordered structures (periodicity, chemistry) on the scattering surface.

II. EXPERIMENTAL

In order to carry out atomic beam scattering from clean single crystal surfaces under optimal conditions, a scattering chamber wherein an ultra high vacuum environment ($< 10^{-8}$ torr) may be maintained during the experiment is required. A cut-away drawing of the bakeable UHV chamber used in this work is shown in Fig. 1. The incident helium beam passes through a gate valve containing a final collimation aperture 1.5 mm in diameter before striking the target surface. After being scattered by the crystal, the beam is detected by a quadrupole mass spectrometer (EAI Model 250-A). Modulated beam techniques and lock-in detection are used to enhance the signal to noise ratio. The detector may be rotated 200° about the sample to obtain the angular distribution of scattered beam and may be raised or lowered to detect scattering out of the plane of incidence (defined by the surface normal and the incident beam direction). A typical angular profile of the incident beam is shown in Fig. 2. The angular

resolution, determined by the size of the collimation slit in the mass spectrometer ionizer, is about 7°. The actual distance between the surface and the ionizer aperture is 2.0 cm while the distance between the final beam collimator and the crystal is 21.5 cm.

Figure 3 shows schematically the major components of the differentially pumped system used to generate the atomic beam. The beam source itself is a multichannel array of capillaries (length/diameter = 100) and may be operated at pressures up to 20 torr without flooding the pumping capacity. Typical operating pressures in the source, selector and scattering chambers are 5×10^{-4} torr, 3×10^{-7} torr, and the low 10^{-9} torr range, respectively. The UHV portion, bakeable to 250°C, is fabricated from 300 series stainless steel and is pumped entirely by sorption and ion pumps to minimize contamination. Conventional, liquid nitrogen trapped diffusion pumps exhaust the other chambers. A vibrating tuning fork (American Time Products Type L40 Light Chopper) was used in the selector chamber to modulate the helium beam in these studies, although it may also be replaced by a rotating disk velocity selector.

By the incorporation of low energy electron diffraction (LEED) optics into the UHV scattering chamber, we are able to monitor in situ the atomic structure of the scattering surface before, during, or after the scattering experiment. Our ability to observe the surface in situ has led to some interesting correlations between observed helium scattering distributions and well characterized surface conditions.

The platinum crystal (MRC, purity 99.999%) used in these studies was prepared by spark cutting a 1 mm thick specimen from a single crystal boule that had been previously oriented to within one half degree of the

(100) direction by back reflection Laue X-ray techniques. Successively finer grades of abrasive, concluding with 0.25μ alumina were used to polish both faces of the crystal until they were parallel to each other within 1°. After this final polish, 0.5 mm thick high purity platinum supports were spot welded to the crystal and a Pt-Pt-10% Rh thermocouple attached to its back surface for use in measuring the sample temperature. The completed assembly was then etched (for fifteen minutes in 50% aqua regia maintained at 100°C) and then thoroughly rinsed (in distilled water and reagent methanol). Following this treatment it was mounted on a Varian Crystal Manipulator and installed in the vacuum system on the axis of the scattering chamber. The crystal could be raised or lowered with respect to the beam line, and could be rotated 360° about an axis bisecting its scattering surface for positioning with respect to the electron, ion, and atomic beams. Elevated sample temperatures were attained through resistive heating via the platinum holders.

Once the UHV system had been pumped down and baked out, the surface of the crystal could be cleaned by ion bombardment sputtering with 300 eV argon ions followed by heating to anneal out surface damage. To keep the surface clean of carbon due to the cracking of ambient hydrocarbons and carbon monoxide, it was found necessary to periodically heat the crystal in 2×10^{-5} torr of O_2 for 30 minutes.

III. SELECTED STRUCTURAL AND CHEMICAL CHARACTERISTICS OF THE PLATINUM (100) CRYSTAL FACE

In any well controlled gas-solid scattering experiment, detailed information concerning the structural and chemical properties of the single crystal surface utilized should be available. Previous low energy electron diffraction[2-4] and Auger spectroscopy[5] studies have revealed that the clean (100) platinum surface is characterized by a surface structure yielding the (5×1) diffraction pattern (to be shown in Fig. 6a). This structure can be explained as a distortion of the surface atoms from a four-fold into a six-fold rotational symmetry. Similar surface phase transformations have been reported for the (100) faces of gold[6-8] and irridium,[9] elements adjacent to platinum in the periodic table.

The most persistent platinum surface contaminant is carbon.[4,5] Trace amounts of this element stabilize the (1×1) surface structure. Upon heating the crystal to above 1100°K however, the carbon orders into a graphite structure, the basal plane being parallel to the platinum surface. The resultant diffraction pattern consists of narrow rings or segmented rings concentric about the (00) reflection and indicates the presence of ordered graphitic domains of random orientation.[3] This diffraction pattern will be shown in Fig. 8a. Heating the platinum crystal in oxygen at 1200°K for 30-60 minutes is sufficient to remove the surface carbon.

Another persistent contaminant of the platinum (100) surface is adsorbed carbon monoxide. Since CO is (a) one of the major constituents of the residual gases in a stainless steel UHV system, and (b) has a sticking probability on clean platinum near unity,[10,11] it posed a serious problem to the studies reported in this paper. Further, as revealed by

entire curve less intense (~0.6%). The intensity decrease may have been due to increased surface roughness resulting in destruction of the phase coherence of the helium beam or to increased out of plane scatter. In this case the crystal yielded no LEED pattern at any voltage, thus indicating considerable disorder in the bulk as well as the surface due to extended ion bombardment. Ion bombardment followed by subsequen annealing is used most frequently to clean and order the freshly prepared sample.

The helium scattering curve from a clean ordered platinum surface exhibiting the (5×1) surface structure is shown in Fig. 6b while the characteristic diffraction pattern is shown in Fig. 6a. The surface was cleaned of adsorbed gases by flashing it to 1000°K between data points. The scattered intensity at the specular angle represents nearly 5% of the total incident beam intensity or an increase of almost an order of magnitude over that observed from an ion bombarded surface. The angular distribution is sharp, but the full width at half maximum (FWHM) is rather large (~18°) as compared to the incident beam width (7).

Helium scattering distributions from other ordered surface structures are shown in Fig. 7b and 8b. The C(4×1) structure, shown in Fig. 7a, yielded specular intensities only slightly lower than those observed from the (5×1) surface structure as indicated by a comparison of Fig. 7b and 6b. This large intensity indicates that surface reconstruction rather than ordered adsorption of low molecular weight gases may be the cause of the formation of this surface structure. Scattering from the graphitic carbon surface structure (Fig. 8b) on the other hand is broader than that from the (5×1) structure and lower in intensity by a factor of two, although it is more than twice as intense as scattering from a platinum surface that had been intentionally contaminated by disordered carbon.

B. Effect of Adsorbed Gases on the Scattering of Helium Beams by a Platinum Surface

Now that we have explored the effects of the surface disorder and the effects of various ordered surface structures on the scattering of helium, let us investigate the effect of adsorbed gases on the nature of helium atom scattering. The scattering curve for helium from a layer of carbon monoxide that is adsorbed on the platinum surface is shown by the open circles in Fig. 9b. As stated earlier CO forms several ordered structures on the (100) face of platinum and at the temperature of this experiment (300°K), CO molecules adsorbed in all three binding states should have been present. The diffraction pattern of this surface (Fig. 9a) was quite diffuse and the broad diffraction spots were barely distinguishable from the background. These conditions indicate a highly disordered chemisorbed surface layer and the helium scattering bears out this contention (Fig. 9b). The specular intensity is quite low (~0.3%) and there is a definite cosine contribution near the surface normal as shown in the open circles.

The weakly bound α-CO molecules can be desorbed hy heating the crystal to 500°K, leaving only the more strongly bound β-CO.[4] A helium scattering distribution obtained in the presence of this tightly bound species is shown by the filled circles in Fig. 9b. Note the striking increase in the specular intensity and the near symmetry of the peak. The cosine contribution has virtually disappeared indicating a greater degree of surface order.

Acetylene, when chemisorbed on the Pt(100) surface gives rise to a C(2×2) diffraction pattern indicative of 50% surface coverage. The diffraction spots are well defined but broad (Fig. 10a) and the high back-

ground intensity reveals a great deal of surface disorder. Again the helium scattering curve (Fig. 10b) confirms this hypothesis. The specular intensity is low (~0.5%) and the intensity peak broad.

C. Effect of Surface Temperature on the Beam Intensity

Finally, the surface temperature dependence of the scattered helium intensity was measured in the range 450°K to 1300°K and the results tabulated in Table I. This experiment has been difficult to carry out in the other beam scattering studies using epitaxial thin films because of the possible changes in surface roughness (sintering) and surface orientation with surface temperature. Similarly, beams scattering studies in non-UHV systems are restricted to elevated surface temperatures on account of surface contamination problems. It can be seen that while there is a decrease in scattered intensity with increasing surface temperature, this decrease is not monotonic as one would expect due to thermal vibrations of surface atoms. The minimum observed at 900°K is very reproducible and probably is due to the adsorption of CO into the β binding state on the (100) face of platinum during the course of the experiment.

V. DISCUSSION

We shall first consider the extent of agreement of the observations reported here with previously published work. Then we shall discuss the results of these studies and the conclusions that can be drawn.

From the data shown in Fig. 6b, 7b, 8b, 9b and 10b, it is apparent that although the beam dispersion varies greatly, helium atoms scatter specularly from platinum single crystal surfaces in the range of gas and surface temperatures investigated. Similar findings have been reported

TABLE I. Temperature Variation of Specular Scattered Helium Intensity

θ_i	Surface Temperature	Scattered Intensity	Ratio
45°	450°K	4.72%	1.00
45°	900°K	2.05%	.44
45°	1125°K	2.32%	.49
45°	1200°K	2.22%	.47
45°	1275°K	2.15%	.45

for helium scattering on epitaxially grown single crystal films of Ag, Ni and Au[16] and on single crystal surfaces of W[17] and Pt[1] Thus it appears that studies that were carried out on oriented thin film deposits reflect the true nature of the atomic scattering process.

Our results have also confirmed the great sensitivity of helium scattering to surface disorder. It appears there is a qualitative correlation between the diffraction spot intensities of the LEED patterns and the fraction of specularly scattered helium atoms. The loss of diffraction features and the corresponding increase in background intensity coincide with the decrease of the maximum specular intensity to below 1% of the incident beam.

A comparison of our helium scattering from the (100) face of platinum crystals with that obtained by Datz, Moore, and Taylor.[18] and Hinchen and Foley[19] using polycrystalline platinum targets reveals certain discrepancies. Both studies yielded cosine-like distributions for scattering from surfaces at 300°K. This would certainly be expected if the platinum surfaces are covered by a disordered layer of low molecular weight gas (viz. Fig. 9). The scattered intensity observed by the other investigators however at higher temperatures (> 500 K) were predominantly backscattered (i.e. the peaks were located between the specular angle and the surface normal.) More recent observations of helium beam scattering on a variety of clean single crystal surfaces,[1,16,17] as well as our own observations for the (100) face of platinum, indicate that the scattered helium peak does not deviate from the specular position as the surface temperature is raised. As has been shown in this paper surface contamination reduces the specular intensity and increases the dispersion of the scattered beam but it does

not shift the scattered beam maximum in the case of helium. Consequently, contamination, even by species diffusing from the bulk, cannot account for the observation. One possible reason for this discrepancy lies in the different topography of the single crystal and polycrystalline surfaces. Experiments conducted during the epitaxial growth of a (111) Au film[20] (in order to maintain a clean surface) have shown that helium scattering from polycrystalline surfaces tends to be somewhat backscattered and is much broader than from a monocrystalline surface of the same material. Similar results were observed with Ni.[16] The presence of grain boundaries, differences in step heights, dislocation and point defect densities may markedly effect the scattered intensity distribution from polycrystalline surfaces. Unfortunately no temperature dependence studies of helium scattering from clean polycrystalline surfaces has yet been reported, so we cannot check our contention that the local microscopic topography of the surface is responsible for the observed angular deviation with temperature.

Our studies indicate that while the scattered helium beam may be useful for monitoring surface disorder, it cannot distinguish well between ordered surface structures of different kinds. Because the intensity maxima for scattering from the (5×1) and C(4×1) structures were nearly of identical magnitude, the helium beam seems relatively insensitive to the periodicity of the scattering lattice. The clean platinum surface and the graphitic carbon surface, however, yielded scattered intensities that were different by a factor of two. This is largely due to the different atomic masses of platinum and carbon (a mass ratio effect), because a calculation of the relative helium scattering intensities from platinum and

graphite surfaces using the hard cube model[21-23] gives roughly a factor of three difference, even though the predicted angle of maximum intensity is incorrect. Thus, while the scattered intensity of the helium beam is slightly sensitive to the chemical nature of the scattering surface, it is probably not selective enough to be experimentally useful.

The temperature dependence of the scattered helium distribution shows a decrease in the maximum intensity of more than fifty percent with increasing temperature in the range of 450°K to 1300°K. Due to increasing thermal disorder with increasing surface temperature, one would expect a monotonic decrease in the specular intensity. The deviation at 900°K from the expected fall off is probably due to the adsorption of the β binding state of CO from the ambient atmosphere. As we stated earlier, this species desorbs near 880°K and the small temperature difference is probably not enough to prevent the gradual readsorption of the gas.

Our observation of the enhanced helium scattering by ordered graphitic carbon seems to be unique. Merrill and Smith[24] have reported no difference in the maximum intensity for helium beams scattered from amorphous and ordered carbon on a platinum (111) surface and they show a drastic increase in the half width (18° → 40°) in going from the amorphous to the ordered state. On the (100) surface there appears to be a slight decrease (40° → 30°) in the half width in going to the ordered surface as would be predicted by our earlier arguments and more than a twofold increase in the intensity maximum. We can advance no satisfactory explanation for this phenomenon other than the inherent differences in the atomic structure of the two crystal planes.

Finally let us consider the differences in the observed half-widths of the helium scattering distributions. On the (111) faces of the fcc metals studied to date, the observed scattered helium peak half-widths increase in order Ni[16] < Pt[1] < Ag[16] < Au[16] which parallels the increase in Debye temperatures for these solids. Smith and Merrill have reported half-widths for helium as small as 8° on the (111) face of platinum.[1] We note that LEED studies of the clean (111) faces of these metals have shown that they do not readily undergo structural rearrangements (reconstruction). The (5×1) surface structure on (100) platinum may, however, represent a rearranged surface with respect to the bulk-like (1×1) unit mesh. There would then be a periodic "buckling" of the surface plane[25] resulting in increased surface roughness which, according to data presented earlier, would yield broadened scattering peaks. Yamamoto and Stickney recently reported on rare gas scattering from a W(100) surface[17] and they found surprisingly broad half-widths (~30°) for helium scattering. Their crystal was cleaned by oxidizing the carbon impurities in 2×10^{-7} torr O_2 at 1300°K with occasional flashes to 2000°K. Germer and May,[26] in studies conducted between 3×10^{-10} and 3×10^{-7} torr of oxygen, have postulated that oxygen atoms are adsorbed into the tungsten lattice by interchange with the W atoms along alternate rows in the surface layer (surface reconstruction). Subsequent heating to temperatures up to 2000°K produces the evaporation of WO_3 and its polymers.[27-29] If this treatment were to leave a rather rough surface that did not have sufficient time to anneal out due to continued reaction with background oxygen ($P_{O_2} \sim 5\times10^{-10}$ torr), the presence of much a rough surface could possibly account for the observed half-widths. The detector used by Yamamoto and Stickney and

that used in this work both had resolutions of 7°.

The use of the low energy electron diffraction in molecular beam-surface scattering studies opens up the possibility for new types of reactive scattering studies. The reaction of the incident beam with adsorbed gases which form ordered surface structures can be studied in addition to their reaction with the clean substrate. Investigations of this type are in progress in our laboratory.

ACKNOWLEDGEMENT

This work was supported by the United States Atomic Energy Commission.

REFERENCES

†National Science Foundation Predoctoral Fellow

1. D. L. Smith and R. P. Merrill, J. Chem. Phys. (1 Nov. 1970, in press).
2. S. Hagstrom, H. B. Lyon, Jr., and G. A. Somorjai, Phys. Rev. Letters 15,491 (1965).
3. H. B. Lyon, Jr. and G. A. Somorjai, J. Chem. Phys. 46, 2539 (1967).
4. A. E. Morgan and G. A. Somorjai, Surface Sci. 12, 405 (1968).
5. P. W. Palmberg, in the Structure and Chemistry of Solid Surfaces, G. A. Somorjai, Ed. (John Wiley, New York, 1969) p. 29-1.
6. D. G. Fedak and N. A. Gjostein, Acta. Met. 15, 827 (1967).
7. P. W. Palmberg and T. N. Rhodin, Phys. Rev. 161, 586 (1967).
8. A. M. Mattera, R. M. Goodman, and G. A. Somorjai, Surface Sci. 7, 26 (1967).
9. J. T. Grant, Surface Sci. 18, 228 (1969).
10. Bernard J. Wood, Noboru Endow, and Henry Wise, J. Catalysis 18, 70 (1970).
11. Stanley E. Fink and R. P. Merrill, Paper delivered at the Eighth Conference on Microbalance Techniques, 1970.
12. A. E. Morgan and G. A. Somorjai, Trans. Am. Crystl. Assoc. 4, 59 (1968).
13. E A. Wood, J. Appl. Phys. 35, 1306 (1964).
14. G. A. Somorjai and H. H. Farrell, Advances in Chemical Physics, Vol. IX, I. Prigogine and Stuart A. Rice, Eds. (Interscience, New York, 1971).
15. R. M. Goodman, (Ph.D. Thesis), University of California, Berkeley, UCRL-19008, (1969).

16. Joe N. Smith, Jr., Howard Saltsburg, and Robert L. Palmer, in Rarefied Gas Dynamics, Leon Trilling and Harold Y. Wachman, Eds., Vol. II, Suppl. 5, (Academic Press, New York, 1969) p. 1141.

17. S. Yamamato and R. E. Stickney, J. Chem. Phys. 53, 1594 (1970).

18. Sheldon Datz, George E. Moore, and Ellison H. Taylor, in Rarefied Gas Dynamics, J. A. Laurman, Ed., Vol. I, Suppl. 2, (Academic Press New York, 1963) p. 347.

19. John J. Hinchen and William M. Foley, in Rarefied Gas Dynamics, J. H. de Leeuw, Ed., Vol. II, Suppl. 3, (Academic Press, New York, 1966) p. 505.

20. J. N. Smith and H. Saltsburg, J. Chem. Phys. 40, 3585 (1964).

21. R. M. Logan and R. E. Stickney, J. Chem. Phys. 44, 195 (1966).

22. R. M. Logan, J. C Keck, and R. E. Stickney, in Rarefied Gas Dynamics, C. L. Brundin, Ed., Vol. I., Suppl. 4, (Academic Press, New York, 1967) p. 49.

23. R. E. Stickney, R. M. Logan, S. Yamamato, and R. E. Stickney, in Fundamentals of Gas-Surface Interactions, H. Saltsburg, J. N. Smith, Jr., and M. Rogers, Eds., (Academic Press, New York, 1967) p. 422.

24. R. P. Merrill and D. L. Smith, Surface Sci. 21, 203 (1970).

25. J. J. Burton and G. Jura, J. Phys. Chem. 71, 1937 (1967).

26. L. H. Germer and J. W. May, Surface Sci. 4, 452 (1966).

27. J. A. Becker, E. J. Becker, and R. G. Brandes, J. Appl. Phys. 32, 411 (1961).

28. J. B. Berkowitz-Mattuck, A. Buchler, J. L. Engelke, and S. N. Goldstein, J. Chem. Phys. 39, 2722 (1963).

29. P. O. Schissel and O. C. Trulson, J. Chem. Phys. 43, 737 (1965).

FIGURE CAPTIONS

1. Cut-away drawing of bakeable ultra high vacuum chamber showing location of LEED optics, ion bombardment gun, molecular beam, and rotating quadrupole mass spectrometer detector. Ion pump (not shown) located on port below optics.
2. Angular profile of unscattered helium beam taken upstream and downstream from crystal position.
3. Schematic diagram of complete molecular beam-surface scattering system.
4. Scanning electron microscope (SEM) photograph of etched Pt(100) surface tilted at 45° to incident electron beam to enhance picture contrast.
5. Helium beam scattering profile from an etched Pt(100) surface.

6a. Diffraction pattern at E = 63 volts of a clean Pt(100) surface showing (5×1) surface structure. Fractional order spots along x and y axes are due to surface domains rotated 90° to one another.

6b. Helium beam scattering profile from surface shown in Fig. 6a.

7a. Diffraction pattern for Pt(100) surface yielding both (5×1) and C(4×1) surface structures. E = 63 volts.

7b. Helium beam scattering profile from surface shown in Fig. 7a.

8a. Ring like diffraction pattern due to randomly oriented islands of graphite on a Pt(100) surface. E = 63 volts.

8b. Helium beam scattering profile from the graphite surface structure shown in Fig. 8a.

9a. Pt(100)-(1×1) diffraction pattern at E = 63 volts due to presence of chemisorbed CO.

9b. Helium beam scattering from CO contaminated Pt(100) surface. Open circles show results in presence of both α and β binding states of CO.

Filled circles indicate data taken after desorbing CO from the α binding state.

10a. Pt(100)-C(2×2) - C_2H_2 diffraction pattern. E = 63 volts.

10b. Helium beam scattering profile from Pt(100) surface covered with chemisorbed acetylene and yielding diffraction pattern shown in Fig. 10a.

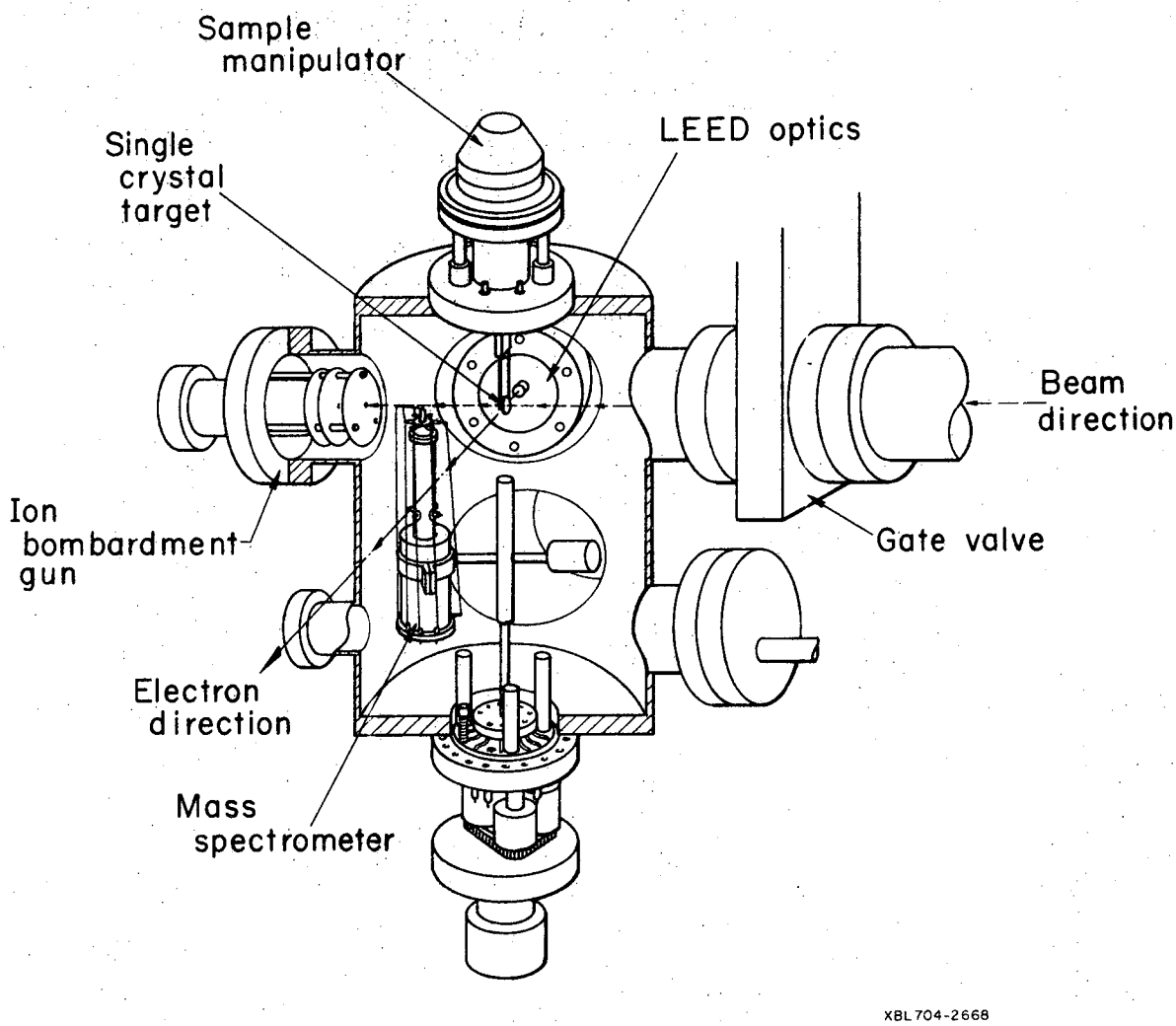

SCATTERING CHAMBER

Figure 1

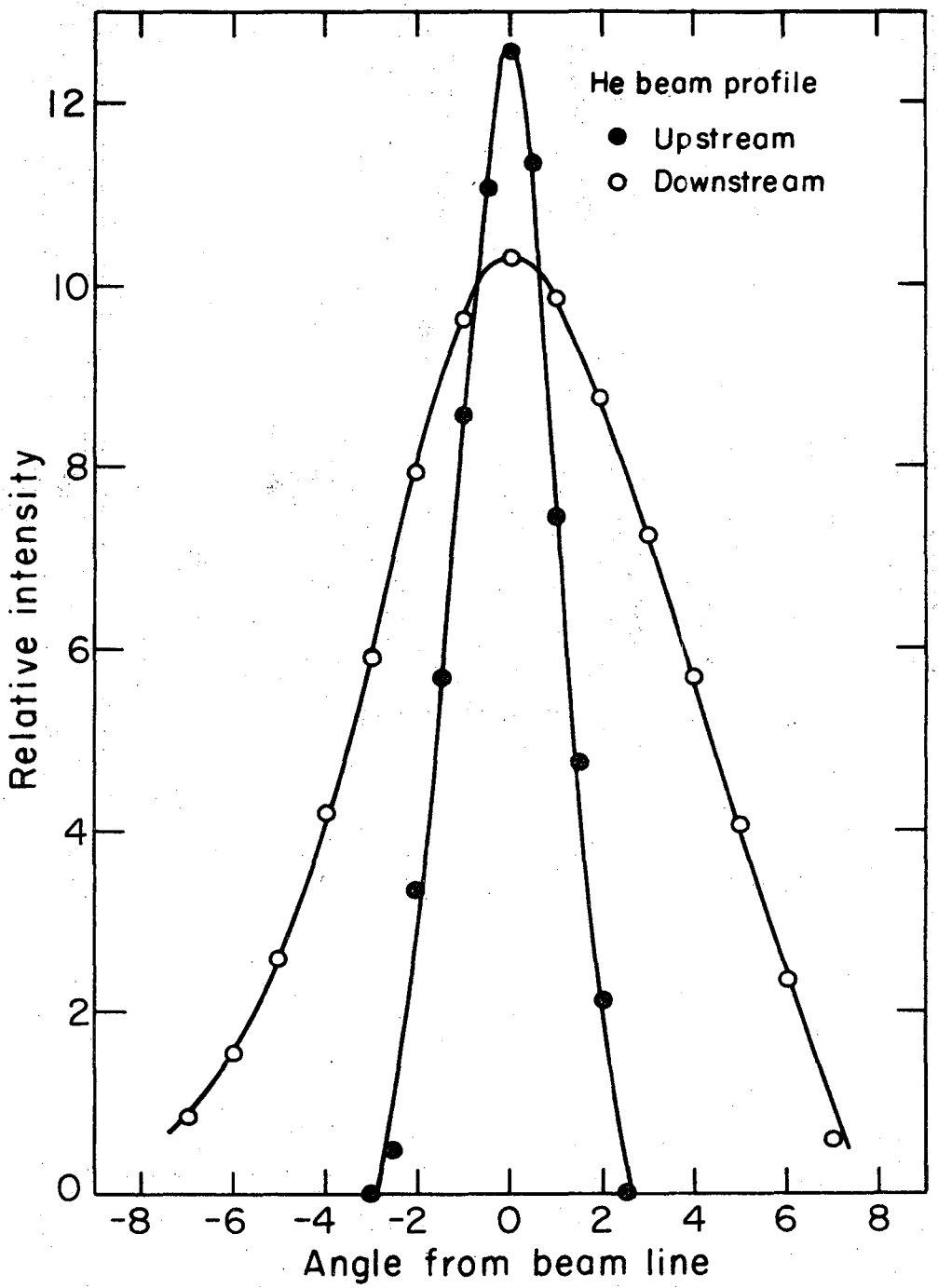

XBL 709-6677

Figure 2

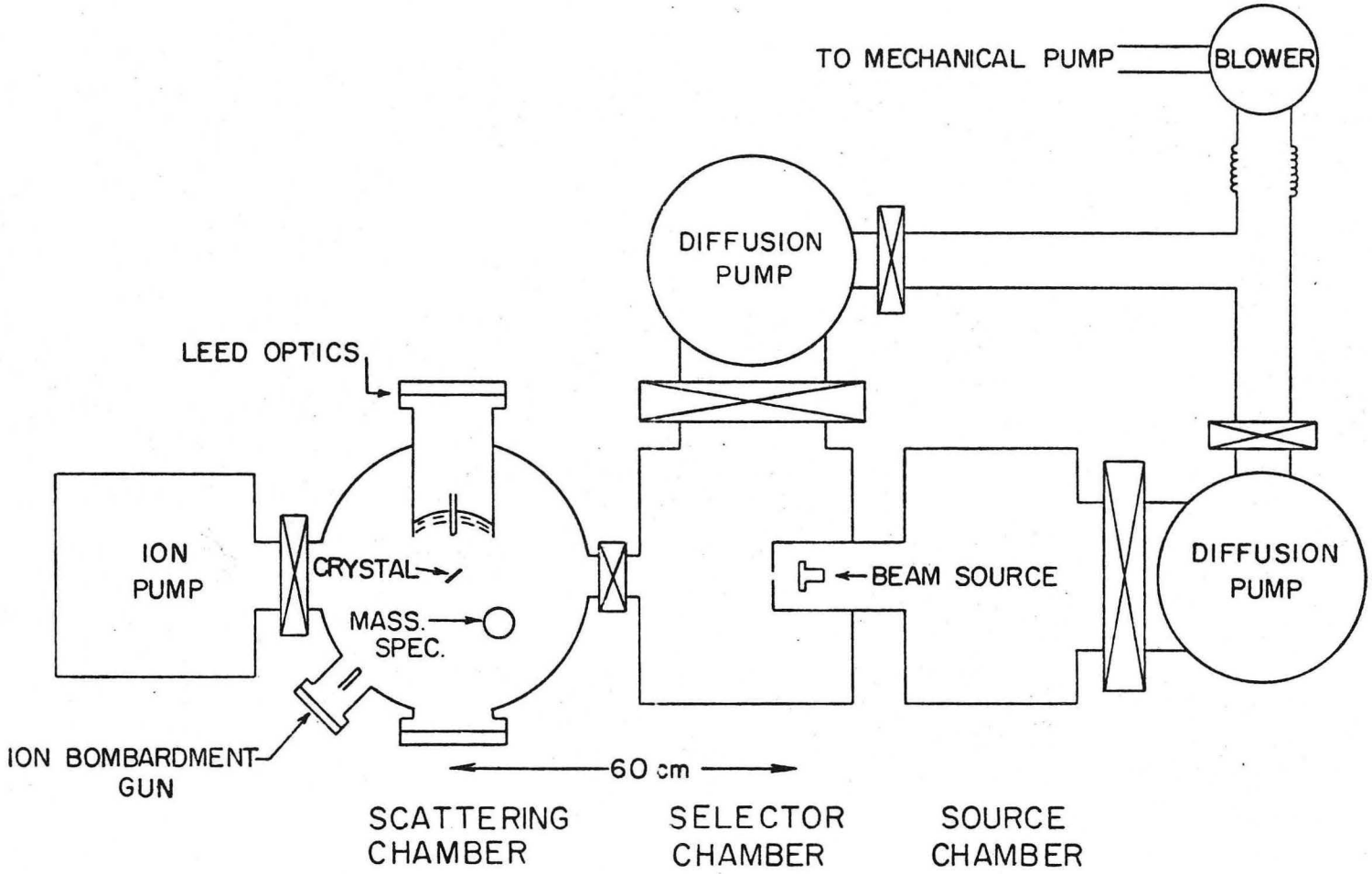

XBL 702-279

Figure 3

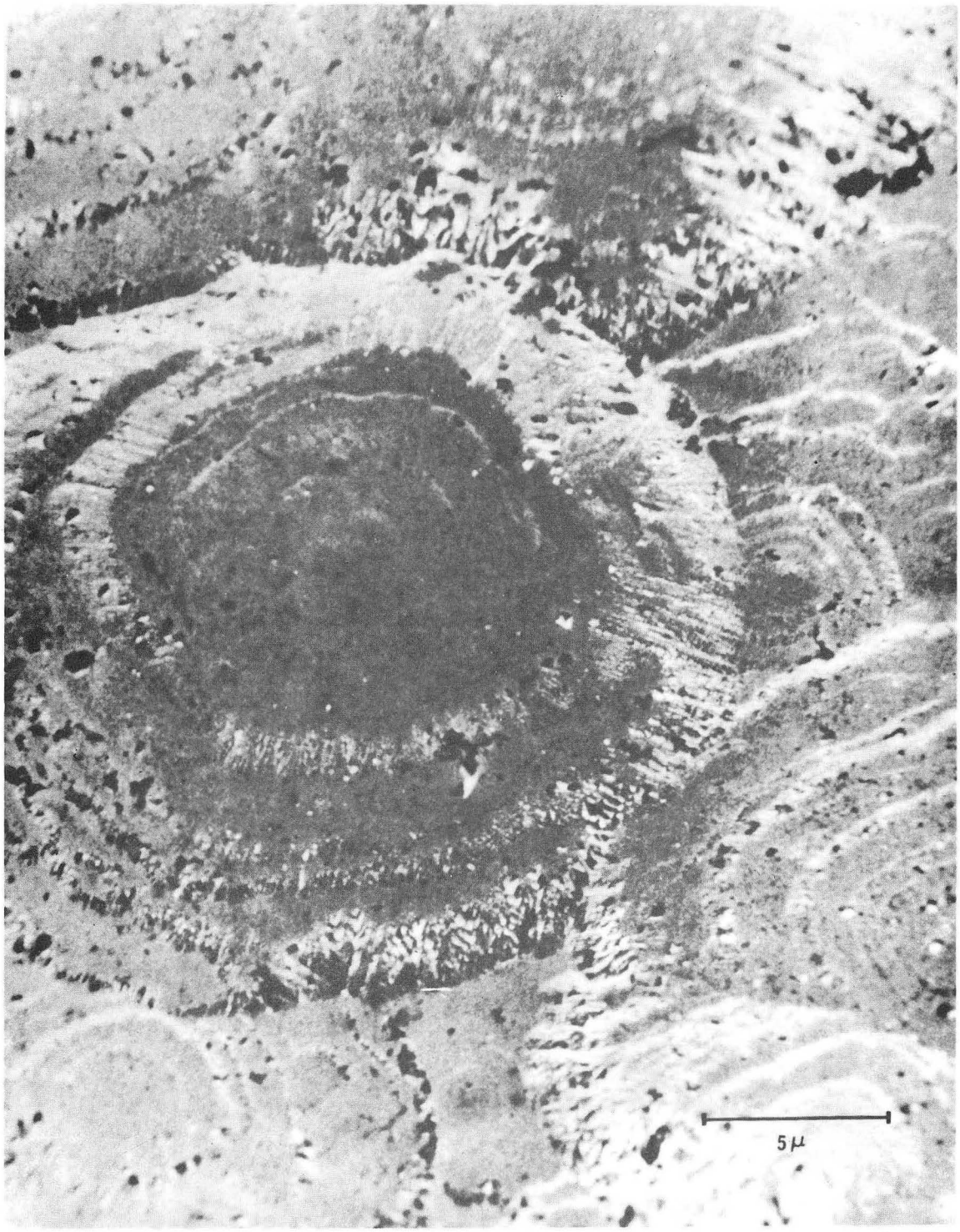

XBB7010-4914

Figure 4

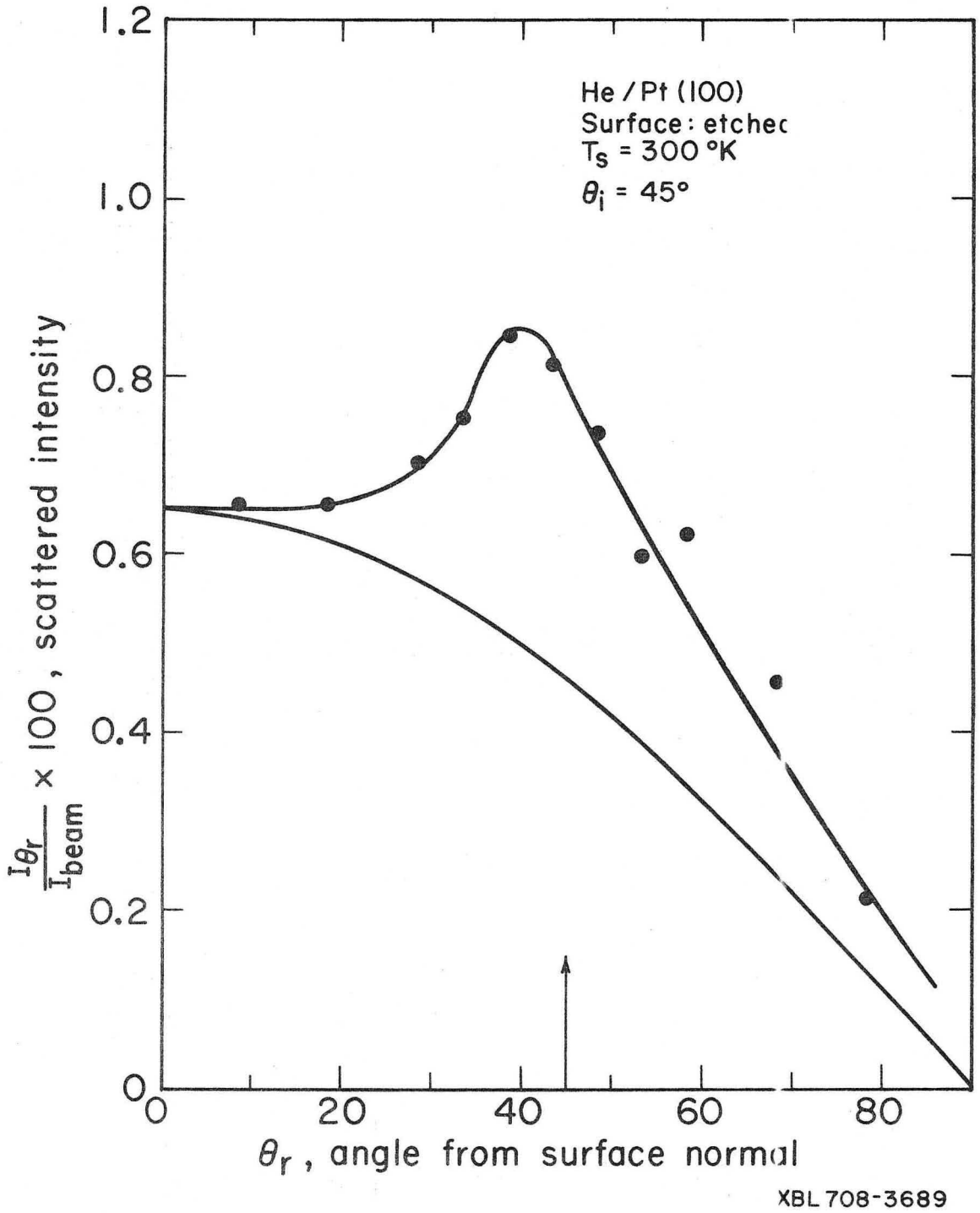
He / Pt (100)
Surface: etched
T_s = 300 °K
θ_i = 45°
$\frac{I_{\theta_r}}{I_{beam}}$ x 100, scattered intensity
θ_r, angle from surface normal
0
0.2
0.4
0.6
0.8
1.0
1.2
0
20
40
60
80
XBL 708-3689

Fig. 5

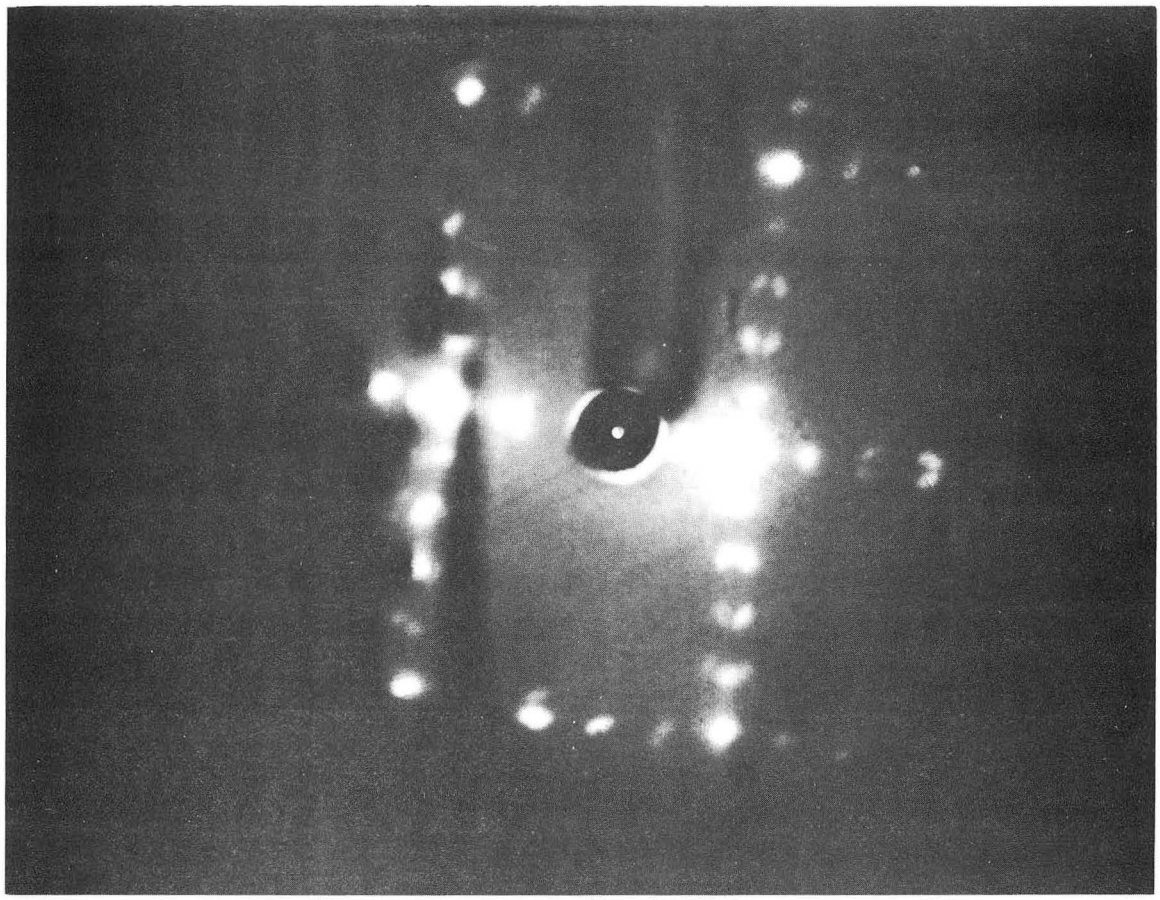

XBB708-3757

Figure 6a

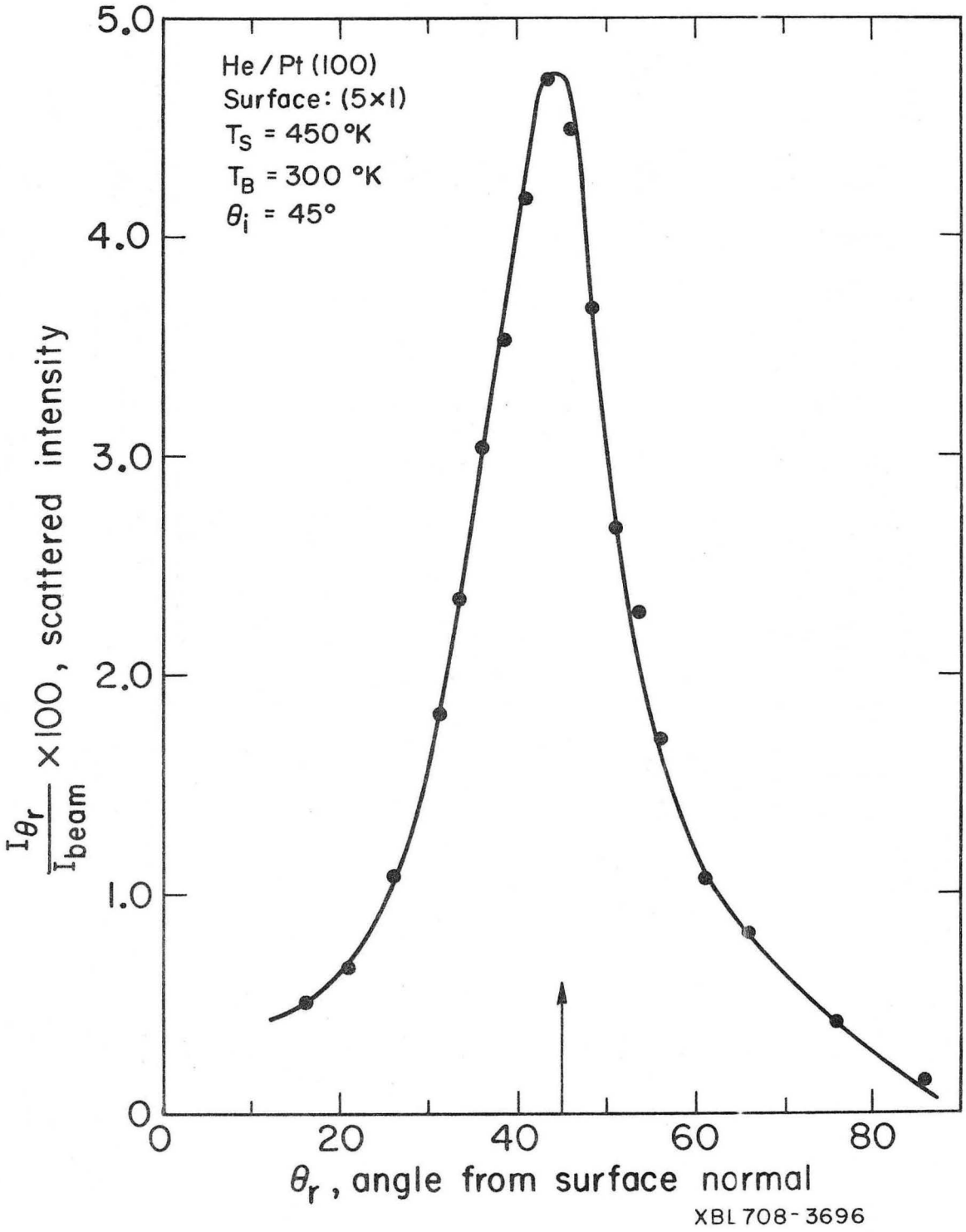
He / Pt (100)
Surface: (5×1)
T_S = 450 °K
T_B = 300 °K
θ_i = 45°
5.0
4.0
3.0
2.0
1.0
0
0
20
40
60
80
$\frac{I_{\theta_r}}{I_{beam}} \times 100$, scattered intensity
θ_r, angle from surface normal
XBL 708-3696

Figure 6b

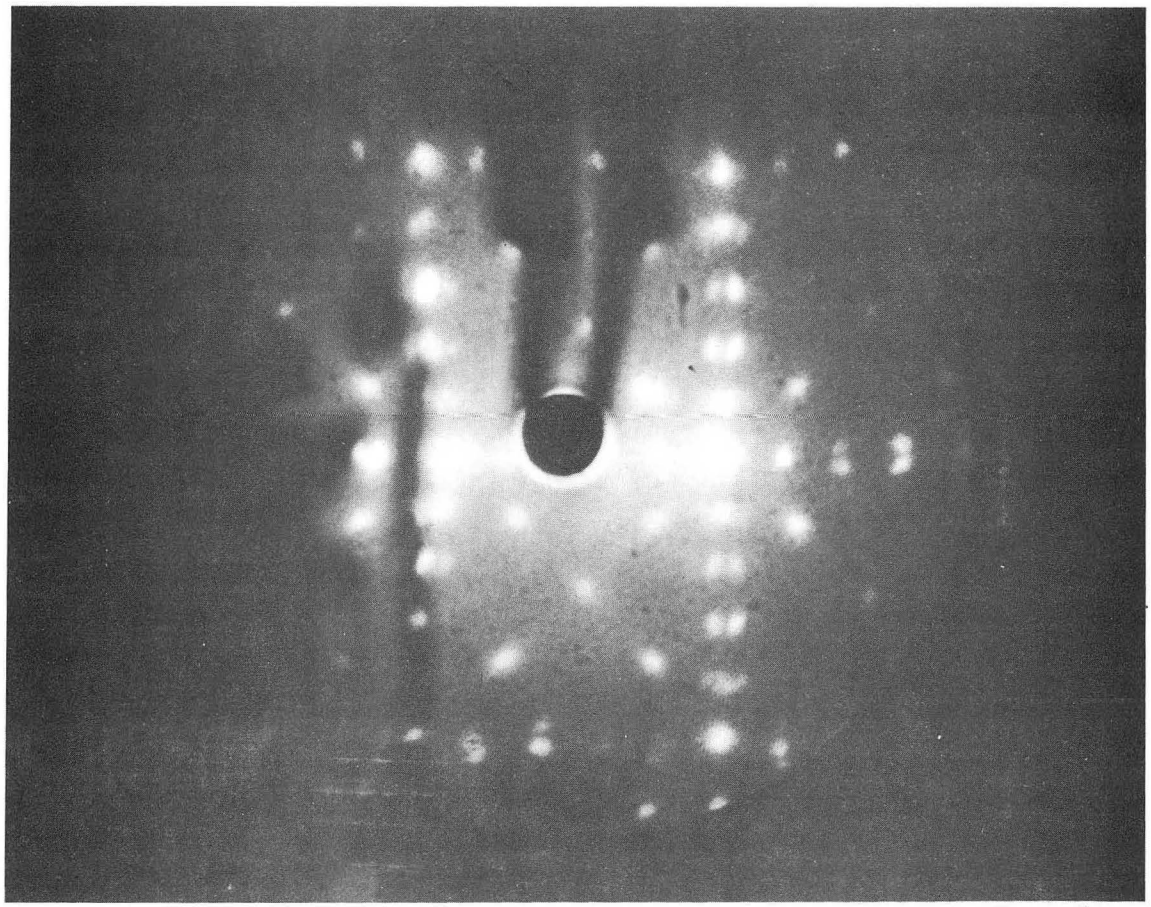

XBB708-3756

Figure 7a

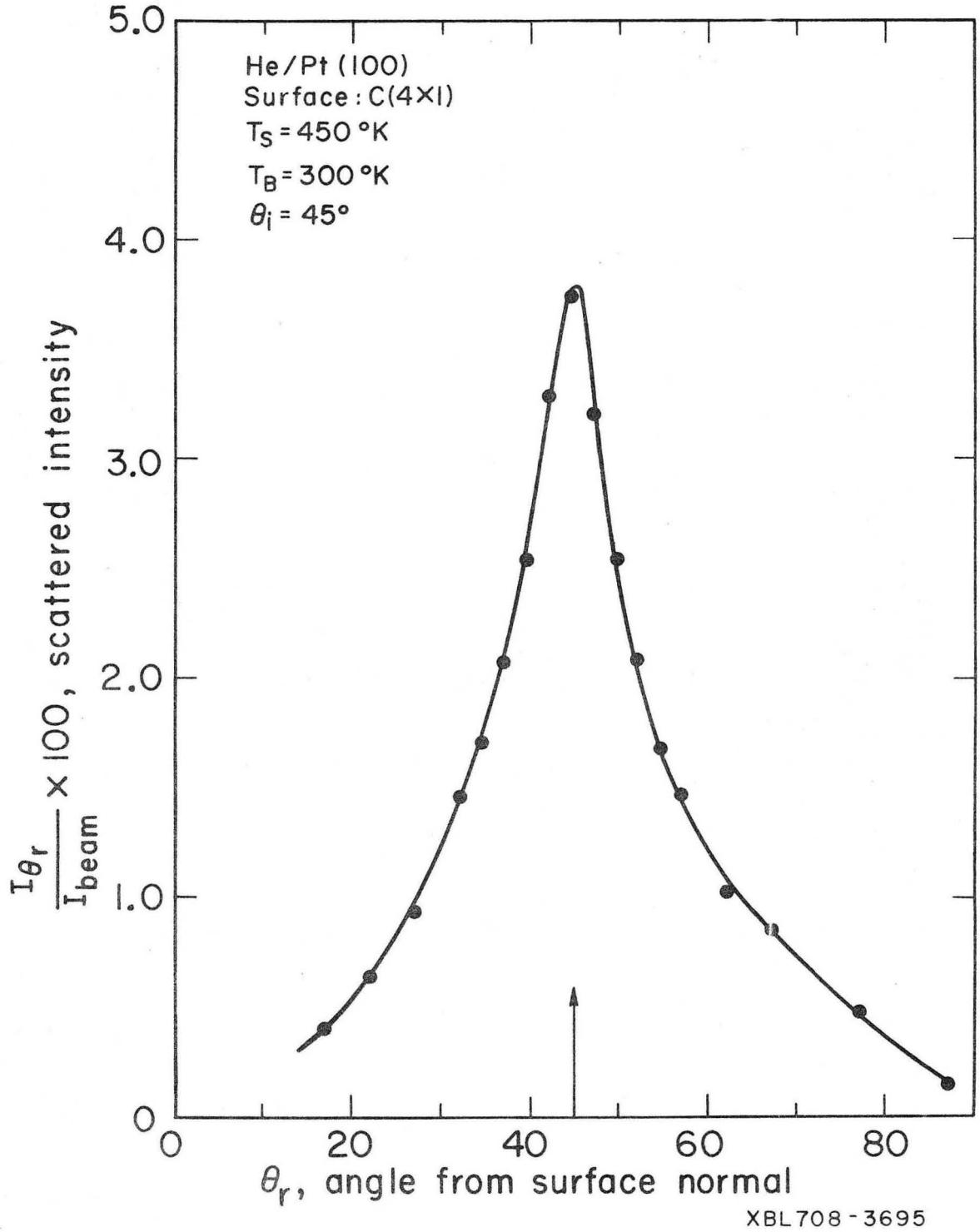
He/Pt (100)
Surface: C(4×1)
T_S = 450 °K
T_B = 300 °K
θ_i = 45°
$\frac{I_{\theta_r}}{I_{beam}} \times 100$, scattered intensity
θ_r, angle from surface normal
0
1.0
2.0
3.0
4.0
5.0
0
20
40
60
80
XBL708-3695

Figure 7b

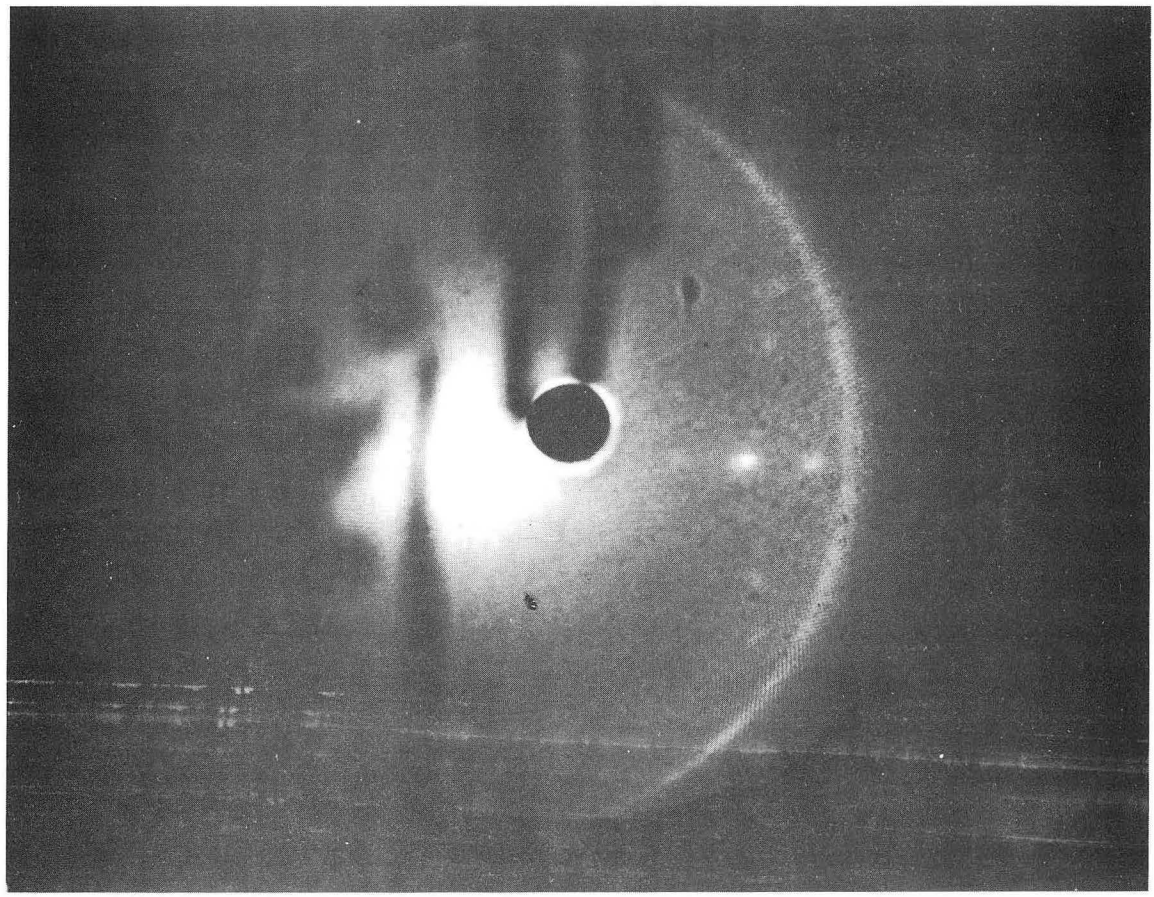

XBB708-3755

Figure 8a

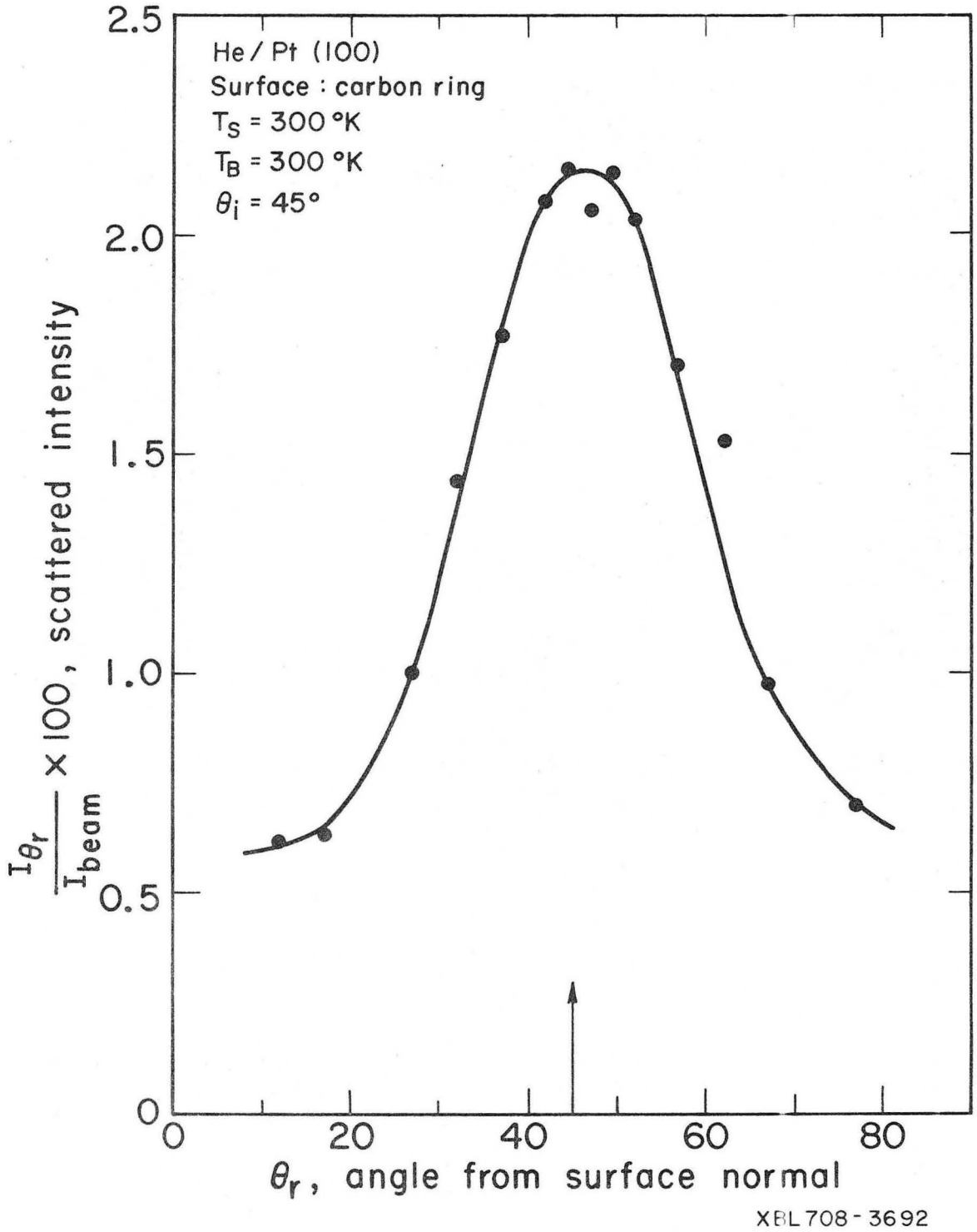
He / Pt (100)
Surface : carbon ring
T_S = 300 °K
T_B = 300 °K
θ_i = 45°
$\frac{I_{\theta_r}}{I_{beam}} \times 100$, scattered intensity
θ_r, angle from surface normal
0
0.5
1.0
1.5
2.0
2.5
0
20
40
60
80
XBL708-3692

Figure 8b

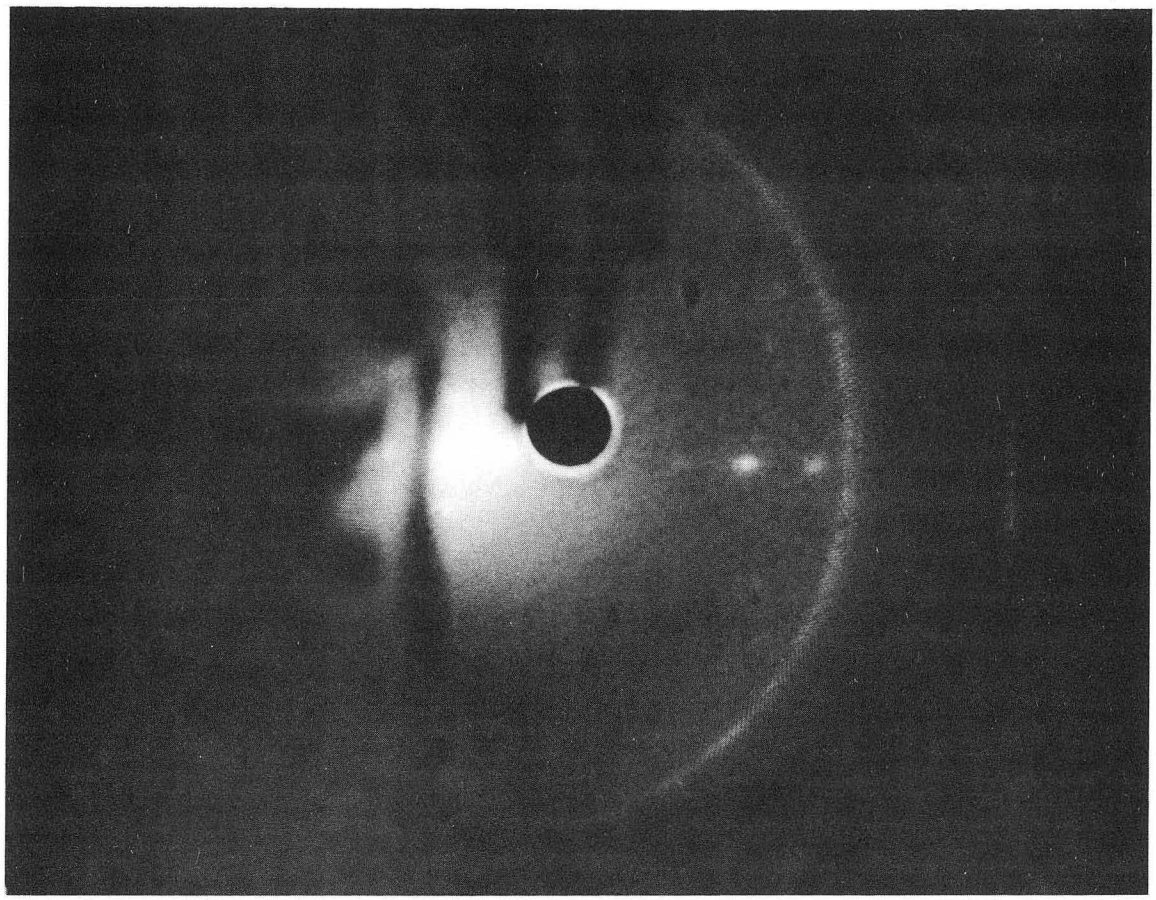

XBB708-3754

Figure 9a

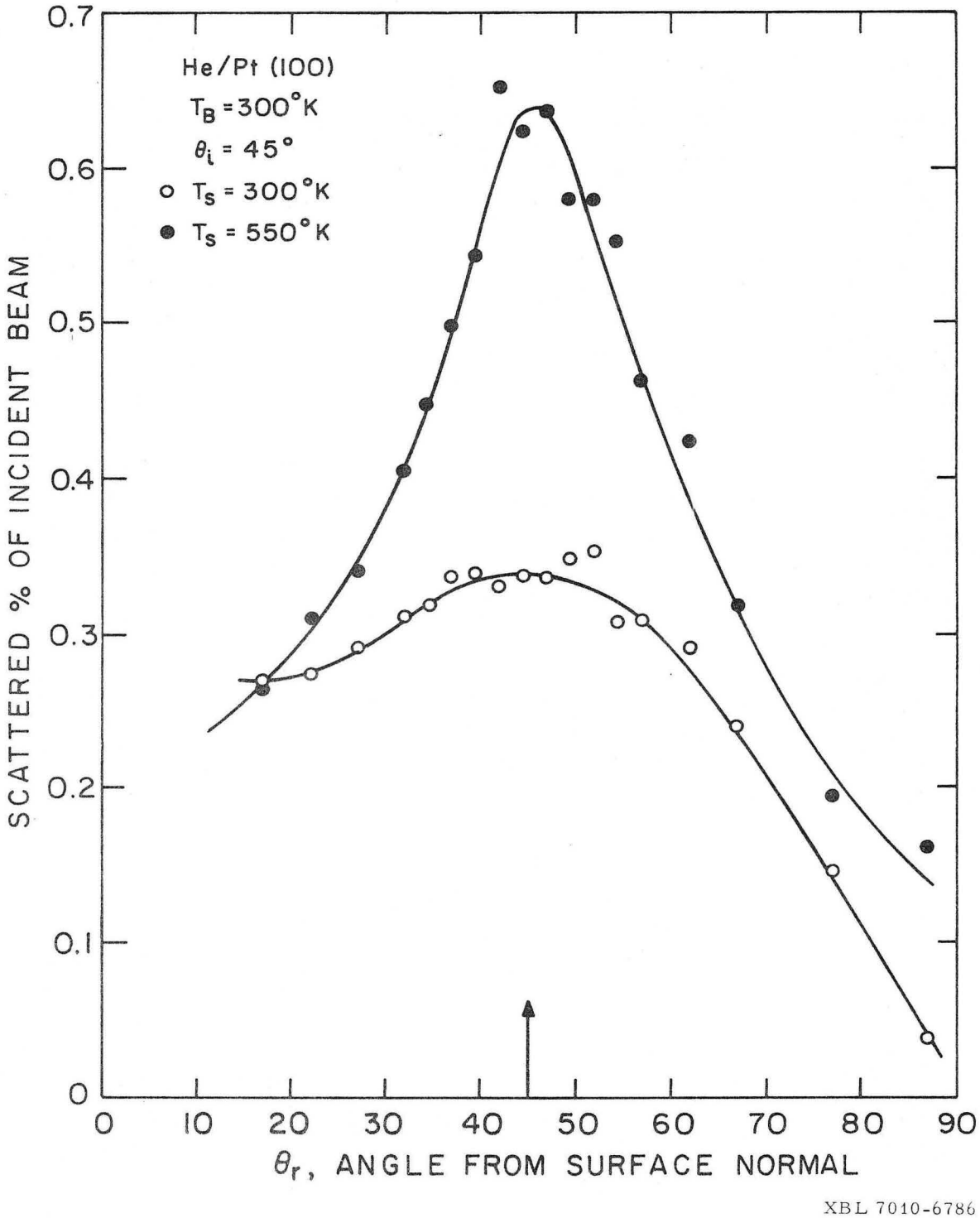
He/Pt (100)
T_B = 300°K
θ_i = 45°
T_S = 300°K
T_S = 550°K
SCATTERED % OF INCIDENT BEAM
0.7
0.6
0.5
0.4
0.3
0.2
0.1
0
0
10
20
30
40
50
60
70
80
90
θ_r, ANGLE FROM SURFACE NORMAL
XBL 7010-6786

Figure 9b

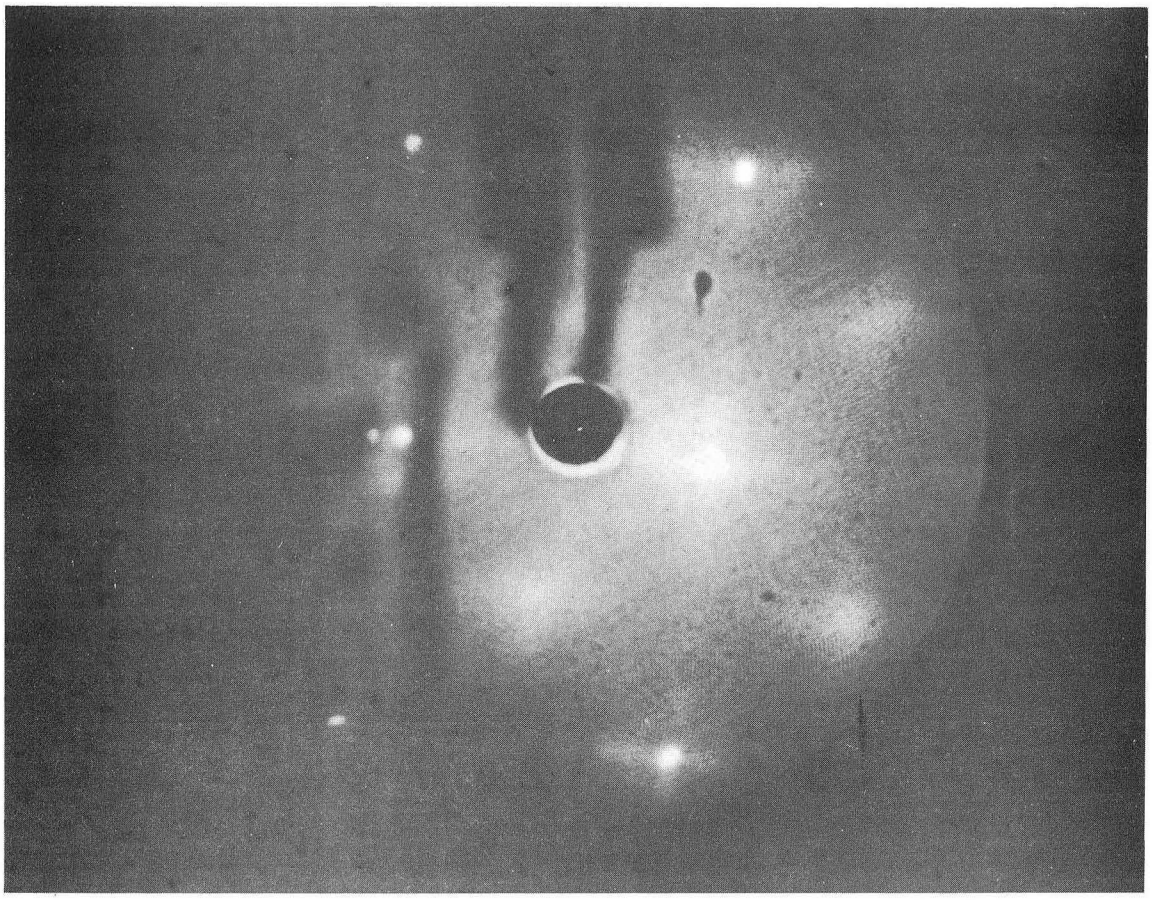

XBB708-3753

Figure 10a

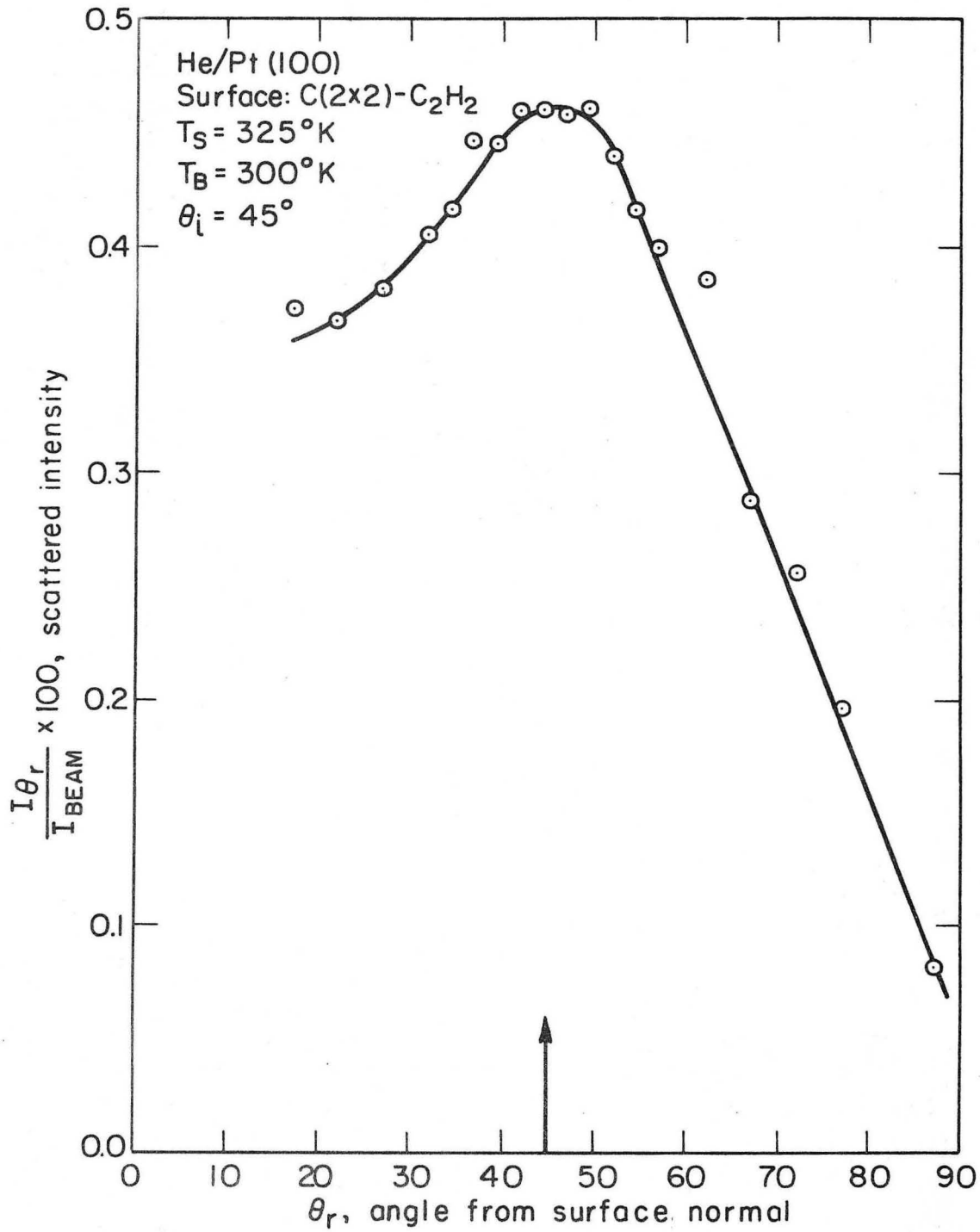

XBL 708-1972

Figure 10b

TECHNICAL INFORMATION DIVISION
LAWRENCE RADIATION LABORATORY
UNIVERSITY OF CALIFORNIA
BERKELEY, CALIFORNIA 94720